Hydro-mechanical Jet Engine's Speed Controller Based on the Fuel's Injection Pressure's Control

ALEXANDRU NICOLAE TUDOSIE
Avionics Department, Faculty of Electrical Engineering
University of Craiova
105 Decebal Blvd., Craiova, jud. Dolj
ROMANIA
atudosie@elth.ucv.ro

Abstract: - The paper deals with an automatic system meant to control an aircraft jet engine's rotation speed, through the fuel injection's control, based on a constant pressure chamber controller. One has established the non-linear mathematical model (based on the motion equations of the system's parts), the linear model and the non-dimensional linear model, as well as the simplified model, the transfer function and the block-diagram. One has also performed a stability study and established the system's stability domains, as well as some quality studies, for different engine-controller configurations.

Key Words: control, jet-engine, fuel injection, pressure chamber, actuator, fuel pump.

1 Introduction

For a gas-turbine engine, particularly for a jet engine, the speed *n* control is one of the most important aspects (even most important than the engine's temperature control) and it's currently realized by some specific hydro-mechanical or electro-mechanical controllers.

The engine's speed is the most important operating parameter, especially for the multi-spool engines, because it represents the parameter which assure the most accurate co-relation with the engine's thrust amount, as well as with the engine's fuel consumption; meanwhile, the speed *n* offers an image about the dynamic load of the engine's mobile parts (compressor's blades and disks, turbine's blades and disks, shafts), as well as an indirect image about the thermal charge of the engine's hot parts (combustor, turbine(s), exhaust nozzle).

An aircraft engine operates at various flight regimes, that means at various flight speed and flight altitudes, which means that the engine's thrust variation must follow the aircraft flight dynamic's necessities, therefore the engine's speed (and thrust) must be strictly controlled, because of its important operating role.

The engine's speed is one of the engine's operating parameters, which are the easiest to measure, both for steady state regimes and for dynamical regimes. That fact represents an advantage and promotes the engine's speed as the most important controlled engine's parameter.

Consequently, any aircraft engine has a speed controller or, at least, a speed limitation gear, in order to assure an optimum operating speed range. Therefore, for the engine's speed control, an important issue is the identifying of the most efficient parameter, which can be used as control parameter during the control activity. There are two important parameters, which have the highest influence above the engine's rotation speed [3,7]:

a) the injected fuel flow rate Q_i;

b) the exhaust nozzle's open area A_5.

The fuel flow rate has a higher influence than the exhaust nozzle's area and it is easier to be itself a controlled parameter, so most of the speed controllers are based on the injected fuel flow rate control, directly or indirectly, using feed-back, feed-before or combined elements.

Possible speed control systems are described in [5, 9,10,11,12], most of them based on feed-back elements, directly measuring the speed values, using mechanical, hydraulic, or electrical sensors or transducers, as well as hydraulic and/or electrical actuators.

Combined controllers (speed and temperature) are forced to operate with the same control parameter, the fuel flow rate, but at different priority levels, that means that one parameter (e.g. the speed *n*), is the main controlled parameter and the other (the combustor temperature or the turbine temperature) is the secondary one ad it is only limited (only its extreme value is controlled), both using the fuel flow rate. Obviously, when the second parameter is limited (by reducing the fuel flow rate), the main parameter is affected too, which represents a disadvantage of such a combined controller, but an acceptable one.

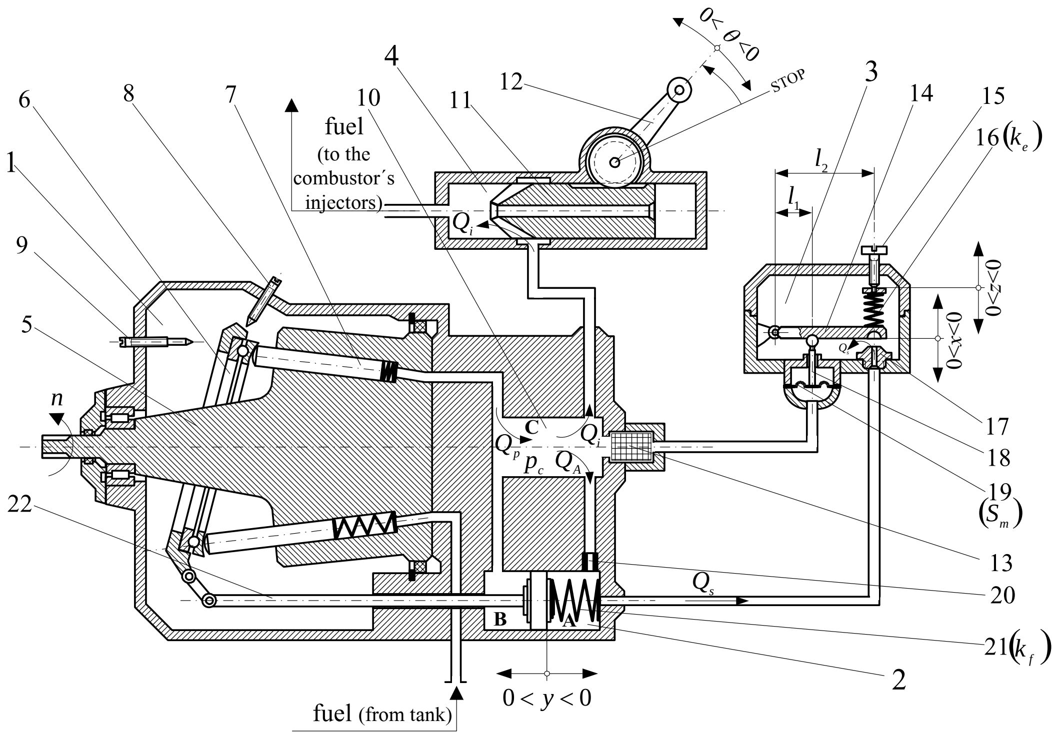

Fig. 1. System's details scheme

In this paper one has studied an engine speed controller with constant pressure chamber, which controls the main fuel flow rate toward the engine's combustor injectors. The system was defined as a controlled object, based on its mathematical model and its transfer function(s) and it was also studied from the stability and quality point of view.

2 Speed controller's presentation

This paper deals with such a controller [10,11], based on the fuel injection pressure's control, in the fuel pump's pressure chamber, before the engine's combustor, as shown in fig.1.

Main parts of the system are: **1**-fuel pump with plungers; **2**-pump's actuator; **3**-pressure sensor with nozzle-flap system; **4**-dosage valve (dosing element).

The fuel pump is connected to the engine's spool, so its rotor 5 has the same speed (or proportional speed) as the engine spool's shaft. The plungers 7 are controlled by the mobile plate 6, which cline angle is established by the actuator's rod 22. The plate's cline limits are established by the tampons 8 and 9, which positions are determining the highest and the lowest level of the injected fuel flow rate; that means that one can set the maximum and the minimum values for the engine's rotation speed by adjusting the tampons' position.

The fuel pump delivers a Q_p fuel flow rate, at a p_c pressure in a pressure chamber 10, which supplies the injector ramp through the dosage valve 4. This dosage valve's slide 11 operates proportionally to the throttle's displacement, being moved by the lever 12. This lever is connected to the engine's throttle, which means that the engine's control lever (throttle) commands the injected fuel flow dosing: a) directly, by the 4 valve's opening; b) indirectly, controlling the pressure's level in chamber 10.

The pump is connected to the engine's rotor's shaft, so its speed is *n*, or proportional to it. Pump's 6 plate's angle is established by the actuator's rod 22 displacement *y*, given by the balance of the pressures in the 2 actuator's chambers (A and B) and the 21 spring's elastic force.

The pressure p_A in chamber A is given by the balance between the fuel flow rates through the drossel 20 and the nozzle 17 (covered by the semi-spherical flap, attached to the sensor's lever 14).

The pressure sensor's lever's displacement *x* is established by the balance between two moments: the first - given by the elastic force of the spring 16 (due to its *z* pre-compression) and the second – given by the elastic force of the membrane 19 (displaced by the pressure in chamber, between the membrane and the fluid oscillations buffer 13).

The system operates by keeping a constant pressure in chamber 10, equal to the preset value

(proportional to the spring 16 pre-compression, set by the adjuster bolt 15).
The engine's necessary fuel flow rate Q_i and, consequently, the engine's speed *n*, is controlled by the co-relation between the p_c pressure's amount and the dosage valve's variable slot dimension (proportional to the lever's angular displacement θ).
A functional block diagram of the system is presented in fig.2.

3 System's mathematical model

System's model is described by a set of non-linear motion equation, but in order to study the system's behavior, some transformation must be done.

3.1 Non-linear model

The non-linear mathematical model consists of the motion equations for each sub-system, as follows:
a) fuel pump flow rate's equation

$$Q_p = Q_p(n, y), \tag{1}$$

b) constant pressure chamber's equation

$$Q_i = Q_p - Q_A, \tag{2}$$

c) fuel pump's actuator's equations

$$Q_A = \mu_{dA} \frac{\pi d_A^2}{4} \sqrt{\frac{2}{\rho}} \sqrt{p_c - p_A}, \tag{3}$$

$$Q_A - Q_s = \beta V_{A0} \frac{\mathrm{d}p_A}{\mathrm{d}t} + S_A \frac{\mathrm{d}}{\mathrm{d}t}\left(y_s + y\right), \tag{4}$$

$$m\frac{\mathrm{d}^2 y}{\mathrm{d}t^2} + \xi \frac{\mathrm{d}y}{\mathrm{d}t} + k_f\left(y_s + y\right) = S_B p_c - S_A p_A, \tag{5}$$

d) pressure sensor's equations

$$Q_s = -\mu_n \pi d_n \sqrt{\frac{2}{\rho}}(z + x)\sqrt{p_A - p_s}, \tag{6}$$

$$l_1 S_m p_c + l_2 \frac{\pi d_n^2}{4} p_A = l_2 k_e (z + x), \tag{7}$$

e) dosing valve equation

$$Q_i = \mu_i b_1 \frac{\theta_s + \theta}{\pi} \sqrt{\frac{2}{\rho}} \sqrt{p_c - p_{CA}}, \tag{8}$$

f) jet engine's equation (for the rotation speed *n*)

$$n = n\left(Q_i, p_1^*, T_1^*\right), \tag{9}$$

where Q_p, Q_i, Q_A, Q_s are fuel flow rates, p_c-pump's chamber's pressure, p_A- actuator's A chamber's pressure, p_{CA}-combustor's internal pressure, p_s-low pressure's circuit's pressure, μ_{dA}, μ_n, μ_i-flow rate co-efficient, d_A, d_n-drossels' diameters, S_A, S_B-piston's surfaces, $S_A \approx S_B$, S_m-sensor's elastic membrane's surface, k_f, k_e-spring elastic constants, V_{A0}-actuator's A chamber's volume, β-fuel's compressibility co-efficient, ρ-fuel's density, ξ-viscous friction c-efficient, *m*-actuator's mobile ensemble's mass, θ-dosing valve's lever's angular displacement (which is proportional to the throttle's displacement), *x*-sensor's lever's displacement, *z*-sensor's spring preset, *y*-actuator's rod's displacement, p_1^*, T_1^* - engine's inlet's parameters (total pressure and total temperature).

3.2 Linear mathematical model

Assuming the small-disturbances hypothesis, one can obtain a linear form of the model; so, assuming that each *X* parameter can be expressed as

$$X = X_0 + \frac{\Delta X}{1!} + \frac{(\Delta X)^2}{2!} + \ldots + \frac{(\Delta X)^n}{n!}, \tag{10}$$

(where X_0 is the steady state regime's *X*-value and ΔX-deviation or static error) and neglecting the terms which contains $(\Delta X)^r, r \geq 2$, one obtains a new form of the equation system, particularly in the neighborhood of a steady state operating regime, as follows:

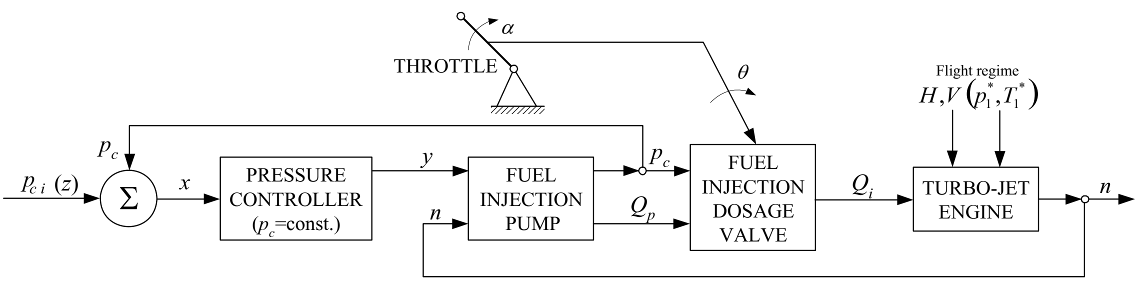

Fig. 2. System's functional block diagram

$$\Delta Q_A = k_A\left(\Delta p_c - \Delta p_A\right), \qquad (11)$$

$$\Delta Q_i = k_{i\theta}\Delta\theta + k_{ic}\Delta p_c\,, \qquad (12)$$

$$\Delta Q_s = k_{SA}\Delta p_A - k_s\Delta x - k_s\Delta z\,, \qquad (13)$$

$$\Delta Q_i = \Delta Q_p - \Delta Q_A\,, \qquad (14)$$

$$\Delta Q_A - \Delta Q_s = \beta V_{A0}\frac{\mathrm{d}}{\mathrm{d}t}\Delta p_A + S_A\frac{\mathrm{d}}{\mathrm{d}t}\Delta y\,, \qquad (15)$$

$$k_e\left(\Delta x + \Delta z\right) = \frac{l_1}{l_2}S_m\Delta p_c\,, \qquad (16)$$

$$\frac{k_f}{S_A}\left(\frac{m}{k_e}\frac{\mathrm{d}^2}{\mathrm{d}t^2}\Delta y + \frac{\xi}{k_e}\frac{\mathrm{d}}{\mathrm{d}t}\Delta y + 1\right) = \Delta p_c - \Delta p_A\,, \qquad (17)$$

where the above used annotations are

$$k_A = \mu_{dA}\frac{\pi\sqrt{2}d_A^2}{8\sqrt{\rho\left(p_{c0} - p_{A0}\right)}},\; k_{i\theta} = \frac{\mu_i b_1\sqrt{2\rho p_{c0}}}{\pi\rho},$$

$$k_{ic} = \frac{\mu_i b_1\left(\theta_s + \theta_0\right)\sqrt{2\rho p_{c0}}}{2\pi\rho p_{c0}},\; k_s = -\frac{\mu_n\pi d_n\sqrt{2\rho p_{A0}}}{\rho},$$

$$k_{SA} = \frac{\mu_n\pi d_n\left(x_0 + z_0\right)\sqrt{2\rho p_{A0}}}{2\rho p_{A0}}. \qquad (18)$$

Using, also, the generic annotation $\overline{X} = \frac{\Delta X}{X_0}$, the above mathematical model can be transformed in a non-dimensional one.

After applying the Laplace transformer to the above determined equations, one obtains the non-dimensional linearised mathematical model, as follows

$$k_{PA}\left(\tau_A\mathrm{s} + 1\right)\overline{p_A} + \tau_y\mathrm{s}\overline{y} + k_{cx}\overline{x} + k_{cz}\overline{z} = \overline{p_c}\,, \qquad (19)$$

$$k_{cx}\overline{x} + k_{cz}\overline{z} = k_{zxc}\overline{p_c}\,, \qquad (20)$$

$$k_{Ay}\left(T_y^2\mathrm{s}^2 + 2\omega_0 T_y\mathrm{s} + 1\right)\overline{y} = k_{AC}\overline{p_c} - \overline{p_A}\,, \qquad (21)$$

$$k_\theta\overline{\theta} + k_{pc}\overline{p_c} - k_{py}\overline{y} = \overline{p_A}\,, \qquad (22)$$

$$k_{cQ}\overline{p_c} - k_{\theta Q}\overline{\theta} = \overline{Q_i}\,. \qquad (23)$$

One must add also the fuel pump equation and the engine's speed equation (having the forms in [9,11])

$$\overline{Q_p} = k_{pn}\overline{n} + k_{py}\overline{y}\,, \qquad (24)$$

$$\left(\tau_M\mathrm{s} + 1\right)\overline{n} = k_c\overline{Q_i} + k_{HV}\overline{p_1^*}\,, \qquad (25)$$

and one obtains the equations of the non-dimensional mathematical model.

Above equation system's co-efficient are

$$k_{PA} = \frac{\left(k_A + k_{SA}\right)}{k_A}\frac{p_{A0}}{p_{c0}},\; k_{cx} = \frac{k_s x_0}{p_{c0}},\; k_{cz} = \frac{k_s z_0}{p_{c0}},$$

$$\tau_A = \frac{\beta V_{A0}}{k_A + k_{SA}},\; \tau_y = \frac{S_A y_0}{k_A p_{c0}},\; k_{Ay} = \frac{k_e y_0}{S_A p_{c0}},\; k_{AC} = \frac{p_{c0}}{p_{A0}},$$

$$T_y = \sqrt{\frac{m}{k_e}},\; 2\omega_0 T_y = \frac{\xi}{k_e},\; k_{zxc} = \frac{k_s S_m p_{c0}}{k_e}\frac{l_1}{l_2},$$

$$k_\theta = \frac{k_{i\theta}\theta_0}{k_A p_{A0}},\; k_{pc} = \frac{\left(k_A + k_{ic}\right)}{k_A}\frac{p_{c0}}{p_{A0}},\; k_{Qp} = \frac{Q_{p0}}{k_A p_{A0}},$$

$$k_{\theta Q} = \frac{k_{i\theta}\theta_0}{Q_{i0}},\; k_{cQ} = \frac{k_{ic}p_{c0}}{Q_{i0}} = k_p\,,$$

$$k_{pn} = \frac{n_0}{Q_{p0}}\left(\frac{\partial Q_p}{\partial n}\right)_0,\; k_{py} = \frac{y_0}{Q_{p0}}\left(\frac{\partial Q_p}{\partial y}\right)_0. \qquad (26)$$

The expressions for τ_M, k_c and k_{HV} are deduced in [12], but here, it isn't necessary to be developed.

Based on this mathematical model, one has built the block diagram in fig. 3.

3.3 Simplified mathematical model

Based on some practical observation, some supplementary hypotheses could be invoked, which are leading to a new form of the mathematical model.

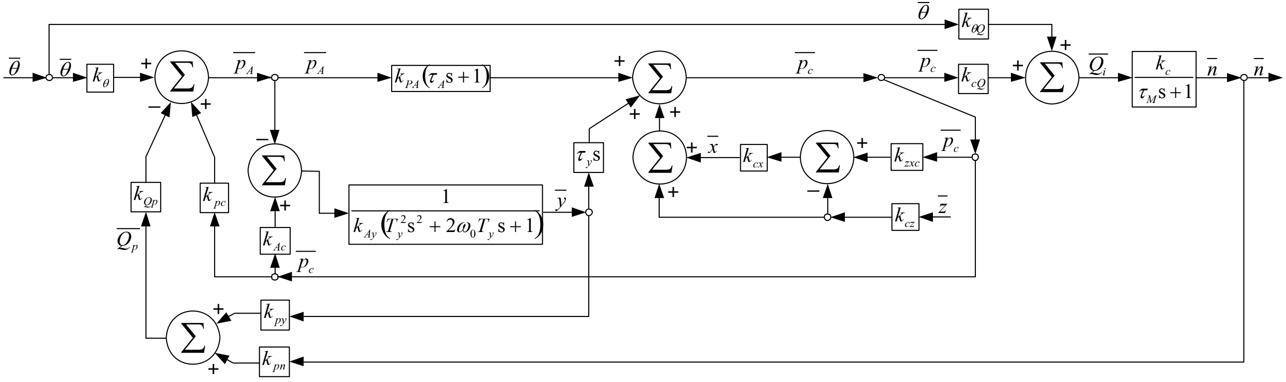

Fig. 3. System's block diagram with transfer functions

These hypotheses are:

a) the fuel is a non-compressible fluid, so $\beta = 0$;

b) the inertial effects are very small, as well as the viscous friction, so the terms containing *m* and ξ are becoming null;

c) the fuel flow rate through the actuator Q_A is very small comparative to the combustor's fuel flow rate Q_i, so it can be neglected, which means that $Q_p \approx Q_i$.

So, the new, simplified, equations' forms, based on these simplifying hypotheses, are:

- for the pressure sensor

$$\bar{x} = k_l\,\overline{p_c} + k_z\bar{z}, \tag{27}$$

where

$$k_l = \frac{p_{c0}}{x_0}\left(\frac{\partial x}{\partial p_c}\right)_0 = \frac{p_{c0}}{x_0}\frac{l_1}{l_2}\frac{S_m}{k_e},\; k_z = \frac{z_0}{x_0}\left(\frac{\partial x}{\partial z}\right)_0, \tag{28}$$

or, considering that the adjusting bolt's displacing represents the preset of the p_c pressure's reference value p_{ci}

$$\overline{p_{ci}} = \frac{k_z}{k_l}\bar{z} = \frac{z_0}{p_{c0}}\left(\frac{\partial p_c}{\partial z}\right)_0,$$

one obtains

$$\bar{x} = -k_l\left(\overline{p_{ci}} - \overline{p_c}\right); \tag{29}$$

- for the actuator

$$(\tau_y s + 1)\bar{y} = -k_x\bar{x}, \tag{30}$$

where τ_y is the actuator's time constant and k_x is the actuator's gain co-efficient with respect to the sensor's lever's displacement. Their forms are, as follows

$$\tau_y = \frac{S_A}{\left(\frac{\partial Q_s}{\partial y}\right)_0 - \left(\frac{\partial Q_A}{\partial y}\right)_0} = \frac{4S_A\sqrt{k_f y_0\left(p_{c0} - k_f y_0\right)}}{k_f\pi\left(2\mu_n d_n x_0 - \mu_{dA} d_A^2\right)}, \tag{31}$$

$$k_x = \frac{\frac{y_0}{x_0}\left(\frac{\partial Q_s}{\partial x}\right)_0}{\left(\frac{\partial Q_s}{\partial y}\right)_0 - \left(\frac{\partial Q_A}{\partial y}\right)_0} = \frac{y_0}{x_0}\frac{4\mu_n d_n p_{A0}\sqrt{k_f y_0}}{2\mu_n d_n x_0 - \mu_{dA} d_A^2}, \tag{32}$$

where $$p_{A0} = p_{c0} - k_f y_0. \tag{33}$$

Introducing these equations into the old mathematical model, one obtains, eventually, its new form, as follows

$$(\tau_M s + 1)\bar{n} = k_c\overline{Q_i} + k_{HV}\overline{p_1^*}, \tag{34}$$

$$\overline{Q_i} \equiv \overline{Q_p} = k_{pn}\bar{n} + k_{py}\bar{y}, \tag{35}$$

$$\bar{x} = -k_l\left(\overline{p_{ci}} - \overline{p_c}\right), \tag{36}$$

$$(\tau_y s + 1)\bar{y} = -k_x\bar{x}, \tag{37}$$

$$\overline{p_c} = \frac{1}{k_p}\overline{Q_i} - \frac{k_\theta}{k_p}\bar{\theta}, \tag{38}$$

which represents the simplified non-dimensional mathematical model.

System's simplified block diagram with transfer function, based on the equations (34) to (38) is presented in fig. 4.

One can observe that the system operates by assuring the constant value of the pressure in the

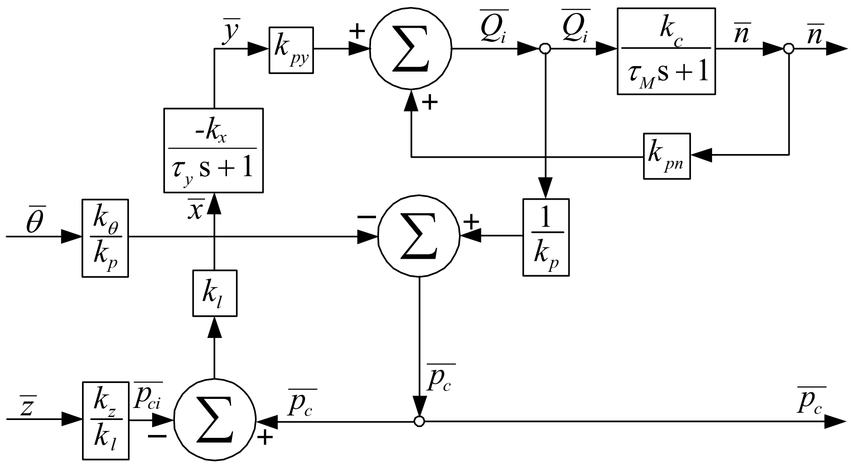

Fig. 4. System's simplified block diagram with transfer functions

fuel pump's chamber p_c, the injection fuel flow rate being controlled through the dosage valve's positioning, which means directly by the throttle. So, the system's relevant output is the pressure in chambers 10, p_c.

For a constant flight regime ($H = \text{const.}, V = \text{const.}$), which means that $p_1^* = \text{const.}, T_1^* = \text{const.}$, the term in Eq. (34) containing $\overline{p_1^*}$ becomes null and the equation's new form is

$$(\tau_M \mathrm{s} + 1)\overline{n} = k_c \overline{Q_i} \ . \qquad (34')$$

3.4 System's transfer function

The last equations, for a constant flight regime, after some appropriate parameters' replacing/reducing, are leading to

$$\left\{\tau_y \tau_M \mathrm{s}^2 + \left[(1 - k_c k_{pn})\tau_y + \left(1 + \frac{k_r k_{py}}{k_p}\right)\tau_M\right]\mathrm{s} + \right.$$

$$\left. + (1 - k_c k_{pn}) + \frac{k_r k_{py}}{k_p}\right\}\overline{p_c} = -\frac{k_\theta}{k_p}(\tau_y \mathrm{s} + 1)(\tau_M \mathrm{s} +$$

$$+ 1 - k_c k_{pn})\overline{\theta} + \frac{k_{py} k_r}{k_p}(\tau_M \mathrm{s} + 1)\overline{p_{ci}} \ , \qquad (39)$$

where $k_r = k_x k_l$.

So, one can define two transfer functions:

a) with respect to the dosage valve's lever angular displacement $H_\theta(\mathrm{s})$;

$$H_\theta(\mathrm{s}) = \frac{-\frac{k_\theta}{k_p}(\tau_y \mathrm{s} + 1)(\tau_M \mathrm{s} + 1 - k_c k_{pn})}{\tau_y \tau_M \mathrm{s}^2 + \left[(1 - k_c k_{pn})\tau_y + \left(1 + \frac{k_r k_{py}}{k_p}\right)\tau_M\right]\mathrm{s} + 1 - k_c k_{pn} + \frac{k_r k_{py}}{k_p}} \qquad (40)$$

b) with respect to the preset reference pressure p_{ci}, or to the sensor's spring's pre-compression z, $H_z(\mathrm{s})$.

$$H_z(\mathrm{s}) = \frac{\frac{k_{py} k_p}{k_p}(\tau_M \mathrm{s} + 1)}{\tau_y \tau_M \mathrm{s}^2 + \left[(1 - k_c k_{pn})\tau_y + \left(1 + \frac{k_r k_{py}}{k_p}\right)\tau_M\right]\mathrm{s} + 1 - k_c k_{pn} + \frac{k_r k_{py}}{k_p}} \qquad (41)$$

While θ angle is permanently variable during the engine's operation (being proportional to the throttle's angular displacement $\overline{\alpha}$), the reference pressure's value is established during the engine's tests, when its setup is made and it remains the same until its next repair or overhaul operation, so $\overline{z} = \overline{p_{ci}} = 0$. Obviously, in this case the transfer function $H_z(\mathrm{s})$ definition has no sense. Consequently, the system's transfer function remains (40), which characteristic polynomial's degree is 2.

4 System's stability

One can perform a stability study, using the Routh-Hurwitz criteria, which are easier to apply because of the characteristic polynomial's form. So, the stability conditions are

$$\tau_y \tau_M > 0 \ , \qquad (42)$$

$$(1 - k_c k_{pn})\tau_y + \left(1 + \frac{k_r k_{py}}{k_p}\right)\tau_M > 0 \ , \qquad (43)$$

$$1 - k_c k_{pn} + \frac{k_r k_{py}}{k_p} > 0 \ . \qquad (44)$$

The first stability condition (42) is obviously, always realized, because both τ_y and τ_M are strictly positive quantities, being time constant of the actuator, respectively of the engine.

In opposite with that, the (43) and (44) conditions must be discussed.

According to [9] and [11], the factor $1 - k_c k_{pn}$ is very important, because its value is the one who gives information about the stability of the connection between the fuel pump and the engine's rotor. There are two situation involving it:

A) $k_c k_{pn} < 1$, when the connection between the engine's fuel pump and the engine's spool shaft is a stable object;

B) $k_c k_{pn} \geq 1$, when the connection between the engine's fuel pump and the engine's spool shaft is an unstable object and it is compulsory to be assisted by a controller.

Both these situations will be analised from the stability and the quality's point of view.

A) ***If*** $k_c k_{pn} < 1$, the factor $1 - k_c k_{pn}$ is strictly positive, so the first term in the left member of (43) is strictly positive, $(1 - k_c k_{pn})\tau_y > 0$.

According to their definition formulas (see annotations (31) and (26)), k_p, k_{py} are positive.

The term k_r must be discussed, because of its denominator. One can assume that, in order to assure a strictly positive value for k_r, between the drossel's diameters d_n and d_A the next relation must be accomplished

$$d_n > \frac{1}{2x_0}\left(\frac{\mu_{dA}}{\mu_n}\right)d_A^2, \tag{45}$$

which represents the first stability request for the controller (a geometrical condition for the drossel's diameter's choice).

The above condition being true, so $\frac{k_r k_{py}}{k_p} > 0$ and $\left(1+\frac{k_r k_{py}}{k_p}\right)\tau_M > 0$, which means that both other stability requests, (43) and (44), are accomplished, thus the system is a stable one for any situation.

B) ***If*** $k_c k_{pn} \geq 1$, the factor $1 - k_c k_{pn}$ becomes a negative one. The inequality (40) leads to

$$\tau_M < \frac{\left(k_c k_{pn} - 1\right)}{\left(1+\frac{k_r k_{py}}{k_p}\right)}\tau_y, \text{ or } \tau_y < \frac{\left(1+\frac{k_r k_{py}}{k_p}\right)}{\left(k_c k_{pn} - 1\right)}\tau_M \tag{46}$$

which offers a criterion for the time constant choice and establishes the boundaries of the stability area (see. Fig. 5).

Obviously, both time constants must be positive, so the domains in fig. 5 are relevant only for the positives sides of τ_y and τ_M axis.

The (45) condition must remain the same.

Meanwhile, from the inequality (44), one can obtain a condition for the sensor's elastic membrane surface area's choice, with respect to the drossels' geometry (d_A, d_n) and quality $\left(\mu_n, \mu_A\right)$, springs' elastic constants $\left(k_e, k_f\right)$, sensor's lever arms $\left(l_1, l_2\right)$ and other stability co-efficient $\left(k_c, k_{pn}, k_{py}\right)$. The (44) inequality becomes

$$S_m > \frac{k_e}{k_f}\frac{l_2}{l_1}\frac{k_c k_{pn} - 1}{k_{py}}\frac{\left(2\mu_n d_n x_0 - \mu_{dA} d_A^2\right)\sqrt{2\rho k_f y_0}}{4\mu d_n p_{A0}}. \tag{47}$$

The above presented inequality (47) is the second geometrical condition for stability, following and completing the (45) condition.

These conditions offers the first pre-design information, concerning the system's stability and can be used as stability estimators.

Another observation can be made, concerning the character of the stability, periodic or non-periodic. If the characteristic equation's discriminant is positive (real roots), than the system's stability is non-periodic type, otherwise (complex roots) the system's stability is periodic type.

Consequently, the non-periodic stability condition is given by the inequality

$$\left[\left(1 - k_c k_{pn}\right)\tau_y + \left(1+\frac{k_r k_{py}}{k_p}\right)\tau_M\right]^2 - \\ - 4\tau_y\tau_M\left(1 - k_c k_{pn} + \frac{k_r k_{py}}{k_p}\right) > 0, \tag{48}$$

which leads to the inequalities

$$\frac{\tau_y}{\tau_M} < \frac{k_p\left(k_c k_{pn} - 1\right)\left(k_r k_{py} - k_p - \sqrt{2\left(k_p^2 + k_r^2 k_{py}^2\right)}\right)}{k_p^2 + k_r k_{py}\left(2k_p + k_r k_{py}\right)}, \tag{49}$$

$$\frac{\tau_y}{\tau_M} > \frac{k_p\left(k_c k_{pn} - 1\right)\left(k_r k_{py} - k_p + \sqrt{2\left(k_p^2 + k_r^2 k_{py}^2\right)}\right)}{k_p^2 + k_r k_{py}\left(2k_p + k_r k_{py}\right)}. \tag{50}$$

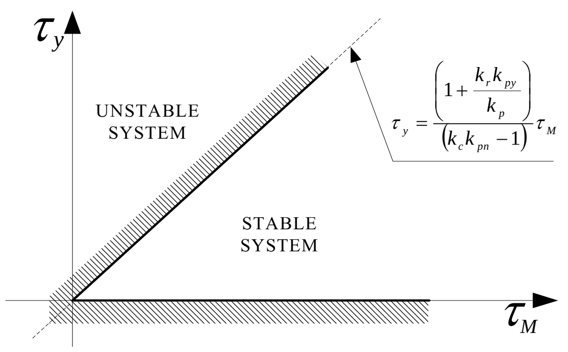

Fig. 5. System's stability domains

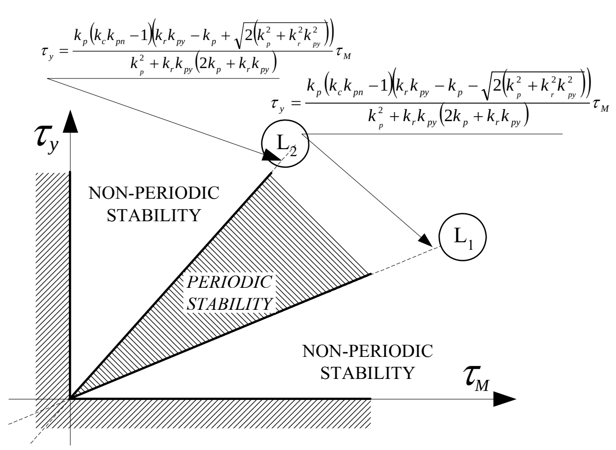

Fig. 6. Periodic and non-periodic stability domains

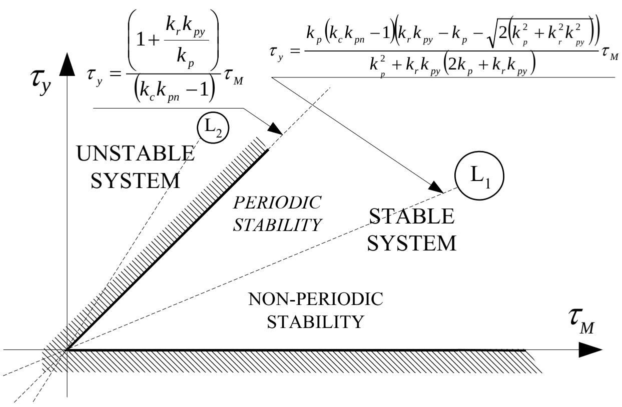

Fig. 7. System's stability domains (for $k_c k_{pn} > 1$)

From the geometrical point of view, as fig. 6 shows, in a $(\tau_y - \tau_M)$ co-ordinate system, these two inequalities are representing two semi-planes, which boundaries are two lines, denoted L_1 and L_2, and given by the equations:

- for L_1

$$\tau_y = \frac{k_p(k_c k_{pn} - 1)\left(k_r k_{py} - k_p - \sqrt{2\left(k_p^2 + k_r^2 k_{py}^2\right)}\right)}{k_p^2 + k_r k_{py}\left(2k_p + k_r k_{py}\right)}\tau_M \quad (51)$$

- for L_2

$$\tau_y = \frac{k_p(k_c k_{pn} - 1)\left(k_r k_{py} - k_p + \sqrt{2\left(k_p^2 + k_r^2 k_{py}^2\right)}\right)}{k_p^2 + k_r k_{py}\left(2k_p + k_r k_{py}\right)}\tau_M \quad (52)$$

In fig. 6 the area between the lines is the periodic stability domain, respectively the areas outside are the non-periodic stability domains.
Both figures (Fig. 5 and 6) are showing the domains for the pump's actuator's time constant choice or design, with respect to the jet engine's time constant. When the domains in Fig. 5 and 6 are overlapped, it results the effective stability map, as fig. 7 shows; one can observe that the left domain of non-periodic stability is, in fact, overlapped on the unstable domain; meanwhile, the stability domain is divided by the line L_1 into the non-periodic and the periodic stability areas.

5 System's quality

As the transfer function form shows, the system is a static one, being affected by static error.
One has studied/simulated a controller serving on an engine Vk-1 type, from the point of view of the step response, which means the system's behavior for step input of the dosage valve's lever's angle θ.
Considering that the engine is operating at the maximum regime, system's time responses, for the fuel injection pressure p_c and for the engine's speed n are

$$\overline{p_c}(t) = \frac{-k_\theta}{k_p + \dfrac{k_r k_{py}}{1 - k_c k_{pn}}}\bar{\theta}(t), \quad (51)$$

$$\bar{n}(t) = \frac{k_\theta k_c k_r}{k_p\left(1 - k_c k_{pn}\right) + k_r k_{py}}\bar{\theta}(t), \quad (52)$$

as shown in fig. 8.a) – for the p_c pressure and in fig. 8.b) – for the engine's speed.
The co-efficient values are calculated for a jet engine Vk-1 type (existing in the Avionics Department of Craiova Labs), using their mathematical expressions and some experimental data (presented in [9], [12] and [11]), for the maximal operating regime (maximum range of the

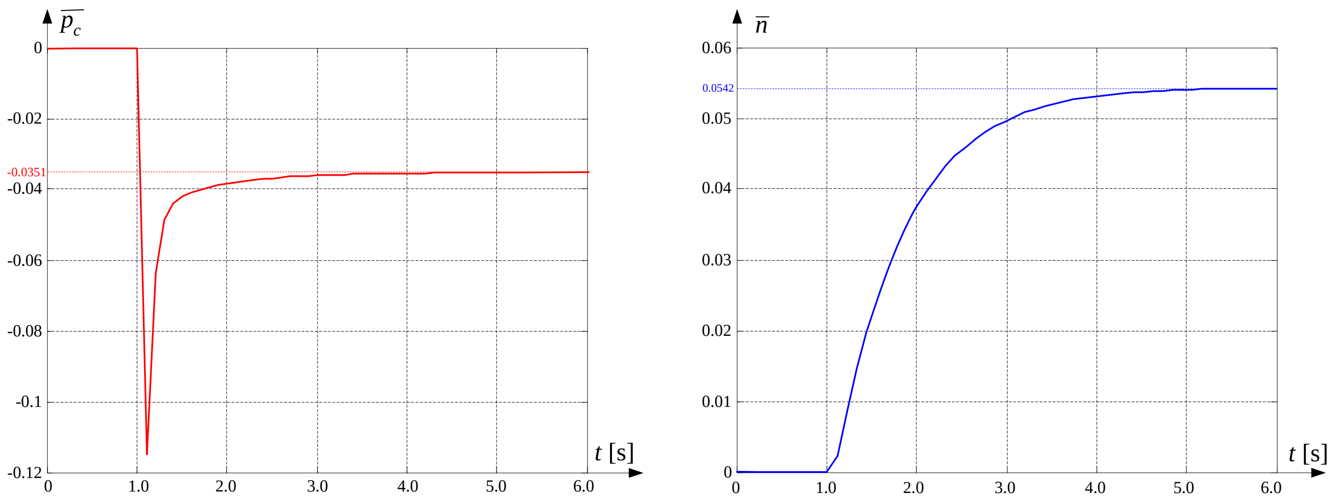

b) b)

Fig. 8. System's step response for $\overline{p_c}$ and $\bar{n}$

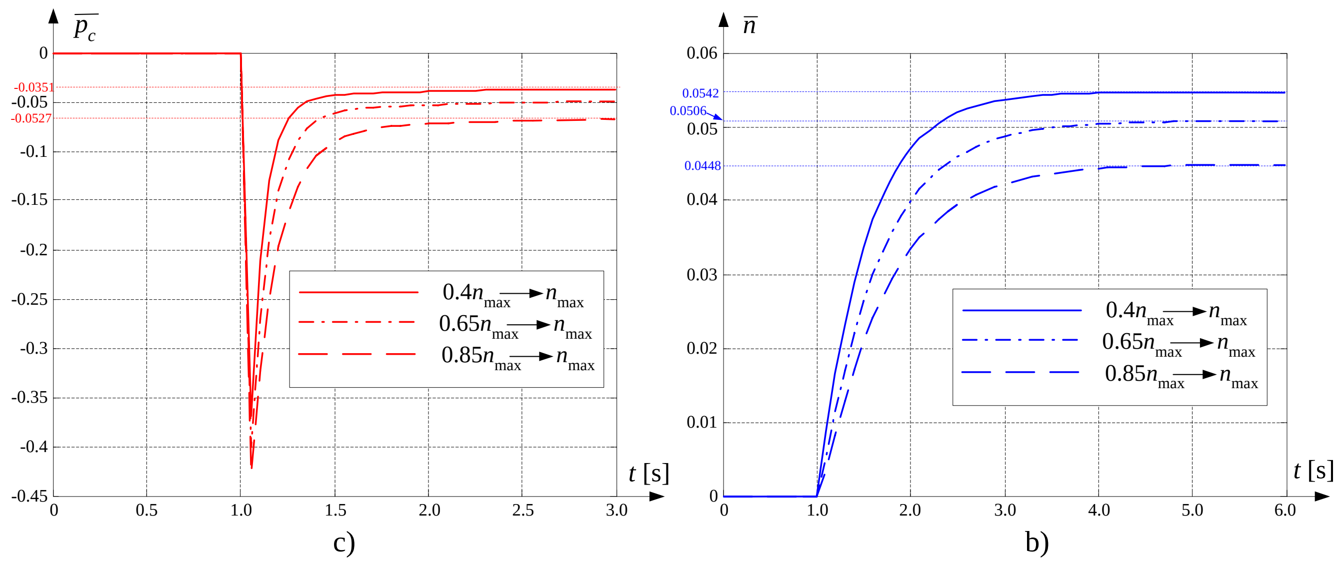

Fig. 9. System's step response ($\overline{p}_c$ and $\overline{n}$) for other engine's operating regimes

engine's acceleration or deceleration).

For the engine's acceleration, from idle to maximum, (assumed as caused by a step input – "step" displacement of the engine's throttle and of the dosing valve's lever), one can observe that the non-dimensional parameter of the pressure $\overline{p}_c(t)$ has an initial step decreasing, $\overline{p}_c(0) = -\frac{k_\theta}{k_p}$ (caused of the rapid dosing valve's slot opening), then an asymptotic increasing; the static error is around 3.5% and it is negative, so the final value of $\overline{p}_c$ is smaller than the prescribed one.

Meanwhile, the engine's speed n is continuous asymptotic increasing, caused by the continuous fuel flow rate's growing. The non-dimensional parameter $\overline{n}$-value's behavior (see fig. 8.b) shows that the static error is around 5.5 %, which is acceptable.

Similarly, one has performed simulations for other engine's operating regimes, such are the partial accelerations (from 65% of the maximum speed to maximum speed, or from 85% of the maximum speed -cruise speed- to maximum speed); the results are presented in fig. 9, together with the results of the full acceleration simulation (from 40 % of maximum speed, which is the idle speed, to maximum speed), already presented in fig. 8. One can observe that, for any operating regime, the trend is the same, any curve $\overline{p}_c(t)$ or $\overline{n}(t)$ having similar shape. The static error decreases from the maximum acceleration regime to the cruise acceleration regime for $\overline{n}$ (from 5.5% to 4.5%), but for $\overline{p}_c$ is increasing (from 3.5% to 5.3%), so the p_c value is as smaller as the acceleration is more intense.

The above discussed simulations were performed for an operating jet engine, a stable controlled system, which co-efficient is $k_c k_{pn} = 0.456 < 1$.

One has also performed simulations for some hypothetic unstable engines, which have such a co-efficient combination that $k_c k_{pn} \geq 1$, respectively an engine which co-efficient value is $k_c k_{pn} = 1.258 > 1$ and an engine which co-efficient value is $k_c k_{pn} = 1.452 > 1$, in this last case the time constant values being close $(\tau_y \approx \tau_M)$. Systems' behavior (step response $\overline{p}_c(t)$ and $\overline{n}(t)$) is presented in fig.10.

Both in this new studied cases, the systems (jet engine+controller) are stable, the studied parameters curves $\overline{p}_c(t)$ and $\overline{n}(t)$ having asymptotic shapes.

In the last case, when $(\tau_y \approx \tau_M)$, its stability happens to be periodic. One can observe that both the pressure and the speed have small overrides (arround 0.85% for n and 0.6% for p_c) during their stabilisation process.

About the static error, one can observe in fig.10.a) that, for $\overline{p}_c$, it changes the sign, becoming positive, and is also growing with the $k_c k_{pn}$-value's growing (from -3.5%, when $k_c k_{pn} = 0.456$, to 5.07% when $k_c k_{pn} = 1.452$).

For the parameter $\overline{n}$, fig. 10.b) shows that the static error is continuous increasing (from 5.5%, when

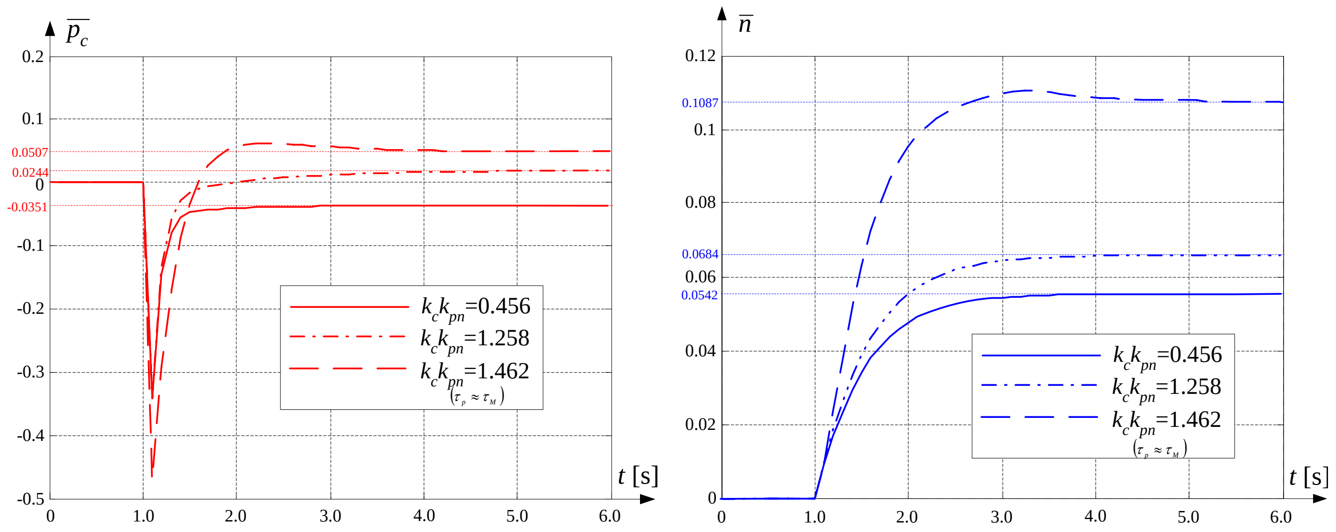

a) b)

Fig. 10. System step response for maximum acceleration of jet engines having different $k_c k_{pn}$ values

$k_c k_{pn} = 0.456$, to 10.9% when $k_c k_{pn} = 1.452$), being unacceptable for this last case, when even the stability is periodic.

6 Conclusions

The studied system (engine+controller) can be characterized as a 2nd order controlled object. For its stability, the most important parameters are engine's and actuator's time constants; a combination of a small τ_y-value and a big τ_M-value (until the stability conditions are accomplished) assures the non-periodic stability, but comparable values $(\tau_y \approx \tau_M)$ can move the stability into the periodic stability domain; a small (or a very small) τ_M value and a big (or a very big) τ_y value are leading, for sure, to instability.

The chosen Vk-1-controller assures both stability and asymptotic non-periodic behavior for the engine's speed, but its using for another engine can produce some unexpected effects.

These studies can be useful for a whole class of similar controllers, as pre-design and pre-operational simulation.

References:

[1] Abraham, R. H. *Complex dynamical systems.* Aerial Press, Santa Cruz, California, 1986.

[2] Aron, I. *Board Equipment for Aircraft*, Tehnica Publisher, Bucharest, 1984.

[3] Krope, J., Dobersek, D., Goricanec, D. - Variation of Pipe Diameters and its Influence on the Flow - Pressure Conditions, *WSEAS Transactions on Fluid Mechanics*, Issue 1, Volume 1, January 2006, pp. 53-59, ISSN 1790-5087.

[4] Lungu, R. *Flight apparatus automation.* Publisher Universitaria, Craiova, 2000.

[5] Mattingly, J. D. *Elements of gas turbine propulsion.* McGraw-Hill, New York, 1996.

[6] Pappas, S. - Robust High Performance Servo Controller Design Technique using Matlab/Simulink, *WSEAS Transactions on Systems and Control*, Issue 2, Volume 1, December 2006, pp. 169-173, ISSN 1991-8763.

[7] Sekozawa, T. - Optimization Control of Low Fuel Consumption Ensuring Driving Performance on Engine and Continuously Variable Trans-mission, *WSEAS Transactions on Systems*, Issue 6, Volume 6, June 2007, pp. 1102-1109, ISSN 1109-2777.

[8] Stevens, B.L., Lewis, E. *Aircraft control and simulation*, John Willey Inc. N. York, 1992.

[9] Stoenciu, D. *Aircraft engine automation. Aircraft engines as controlled objects.* Publisher of Military Technical Academy, Bucharest, 1977.

[10] Stoenciu, D. *Aircraft engine automation. Album with automation schemes.* Publisher of Military Technical Academy, Bucharest, 1977.

[11] Stoicescu, M., Rotaru, C. *Turbo-jet engines. Characteristics and control methods.* Publisher Military Technical Academy, Bucharest, 1999.

[12] Tudosie, A. *Aerospace propulsion systems automation.* Inprint of the University of Craiova, 2005.